Traffic Flow Reconstruction between PDEs and Machine Learning

Nail Baloul, Amaury Hayat, Thibault Liard, Pierre Lissy[1]

MOD Seminar, XLIM, Limoges

October, 10th 2025

[1]N. Baloul, A. Hayat, and P. Liss y are with CERMICS, École nationale des ponts et chaussées, France
Thibault Liard is with XLIM, Université de Limoges, France

Table of Contents

Motivation

Traffic jam in Beijing

- Traffic congestion is a main contributor of air pollution and excessive travel time
  $\Rightarrow$ impacts urban mobility and environmental quality

Motivation

Traffic jam in Beijing

- Traffic congestion is a main contributor of air pollution and excessive travel time
  $\Rightarrow$ impacts urban mobility and environmental quality
- Traffic management relies on **control** schemes to address perturbed traffic conditions
- Most existing control techniques require complete and accurate knowledge of state
- In practice, full information is rarely available due to limited and noisy measurements

Motivation

Traffic jam in Beijing

- Traffic congestion is a main contributor of air pollution and excessive travel time
  $\Rightarrow$ impacts urban mobility and environmental quality
- Traffic management relies on **control** schemes to address perturbed traffic conditions
- Most existing control techniques require complete and accurate knowledge of state
- In practice, full information is rarely available due to limited and noisy measurements
- **Goal** $\Rightarrow$ develop reliable methods for **estimating traffic from partial data**

Traffic Flow Modeling Scales

Benchmark scales of traffic models

- microscopic $\Rightarrow$ individual vehicle dynamics, full information given

Microscopic model

- Simulation of agent-based dynamics
- Tracking position $x_i(t)$, velocity $v_i(t)$ of vehicle i at time t
- Each driver responds to surrounding traffic by adjusting his speed

$$\dot{v}_i(t) = F(v_i(t), x_i(t)) \qquad (1)$$

[2] Di Francesco, Fagioli, Rosini, and Russo 2016.

Traffic Flow Modeling Scales

Benchmark scales of traffic models

- macroscopic $\Rightarrow$ continuum representation using aggregated variables

Macroscopic model

- Traffic modelled as a continuous flow
- Density $\rho(t,x)$, speed $v(\rho)$, flux $f(\rho)$
- Total number of cars is conserved

$$\begin{aligned} 0 =& \frac{d}{dt}\int_a^b \rho(t,x)dx \\ =& f(\rho(t,a)) - f(\rho(t,b)) \\ =& -\int_a^b \frac{\partial}{\partial x} f(\rho(t,x))dx \end{aligned} \tag{2}$$

[2] Di Francesco, Fagioli, Rosini, and Russo 2016.

Traffic Flow Modeling Scales

Benchmark scales of traffic models

- microscopic $\Rightarrow$ individual vehicle dynamics, full information given
- macroscopic $\Rightarrow$ continuum representation using aggregated variables

Microscopic model

- Simulation of agent-based dynamics
- Tracking position $x_i(t)$, velocity $v_i(t)$ of vehicle i at time t
- Each driver responds to surrounding traffic by adjusting his speed

$$\dot{v}_i(t) = F(v_i(t), x_i(t)) \qquad (1)$$

Macroscopic model

- Traffic modelled as a continuous flow
- Density $\rho(t,x)$, speed $v(\rho)$, flux $f(\rho)$
- Total number of cars is conserved

$$\begin{aligned} 0 =& \frac{d}{dt}\int_a^b \rho(t,x)dx \\ =& f(\rho(t,a)) - f(\rho(t,b)) \qquad (2) \\ =& -\int_a^b \frac{\partial}{\partial x} f(\rho(t,x))dx \end{aligned}$$

- **Connection** $\Rightarrow$ macroscopic variables emerge from microscopic interactions[2]

[2] Di Francesco, Fagioli, Rosini, and Russo 2016.

Microscopic Model

- 2 quantities -which only depends on time- used to describe traffic systems
  $\Rightarrow$ state x_i (position of vehicle i at time t)
  $\Rightarrow$ velocity v_i (speed of vehicle i at time t)

Microscopic Model

- 2 quantities -which only depends on time- used to describe traffic systems
  $\Rightarrow$ state x_i (position of vehicle i at time t)
  $\Rightarrow$ velocity v_i (speed of vehicle i at time t)
- Dynamics depend on **headway** $\Rightarrow$ captures reaction effects explicitly

$$\dot{x}_i(t) = v(z_i(t)) \tag{3}$$

where $z_i(t)$ accounts for surrounding of vehicle i

Macroscopic Model

- 3 quantities -which all depend on space and time- used to describe traffic systems
  $\Rightarrow$ relative density ρ (number of vehicles per unit of length)
  $\Rightarrow$ average velocity v (mean speed of vehicles on a road segment)
  $\Rightarrow$ flow rate f (number of vehicles passing across a portion of the road during a period of time)

Macroscopic Model

- 3 quantities -which all depend on space and time- used to describe traffic systems
  $\Rightarrow$ relative density ρ (number of vehicles per unit of length)
  $\Rightarrow$ average velocity v (mean speed of vehicles on a road segment)
  $\Rightarrow$ flow rate f (number of vehicles passing across a portion of the road during a period of time)
- **Fundamental diagram** of traffic flow $\Rightarrow f(\rho) = \rho V(\rho)$

Macroscopic Model

- 3 quantities -which all depend on space and time- used to describe traffic systems
  $\Rightarrow$ relative density ρ (number of vehicles per unit of length)
  $\Rightarrow$ average velocity v (mean speed of vehicles on a road segment)
  $\Rightarrow$ flow rate f (number of vehicles passing across a portion of the road during a period of time)
- **Fundamental diagram** of traffic flow $\Rightarrow f(\rho) = \rho V(\rho)$
- **Hydrodynamic equation** and **conservation law** lead to LWR model

$$\rho_t + (\rho V(\rho))_x = 0 \tag{4}$$

where $V(\rho)$ is the **equilibrium** velocity
$\Rightarrow$ assumes that in any given situation, vehicles immediately adjust their velocity to match the equilibrium velocity dictated by density $v(t, x) = V(\rho)$
$\Rightarrow$ neglects acceleration effects and assumes traffic flow behaves as a compressible fluid

Table of Contents

Model-Based Approaches

- Follow-the-Leader (FtL), **microscopic** first order model
  $\Rightarrow$ dynamics of each vehicle depend on vehicle immediately in front

$$\begin{cases} \dot{x}_N^N(t) = v_{\max}, & t > 0, \\ \dot{x}_i^N(t) = v\left(\frac{L}{N(x_{i+1}^N(t) - x_i^N(t))}\right), & t > 0, \quad i = 0, \cdots, N-1 \\ x_i^N(0) = \bar{x}_i^N, & i = 0, \cdots, N \end{cases} \tag{5}$$

  $\Rightarrow$ accurate traffic representation, encodes individual movements
  $\Rightarrow$ computationally demanding, requires more data

Model-Based Approaches

- Follow-the-Leader (FtL), **microscopic** first order model
  $\Rightarrow$ dynamics of each vehicle depend on vehicle immediately in front

$$\begin{cases} \dot{x}_N^N(t) = v_{\max}, & t > 0, \\ \dot{x}_i^N(t) = v\left(\frac{L}{N(x_{i+1}^N(t) - x_i^N(t))}\right), & t > 0, \quad i = 0, \cdots, N-1 \\ x_i^N(0) = \bar{x}_i^N, & i = 0, \cdots, N \end{cases} \tag{5}$$

  $\Rightarrow$ accurate traffic representation, encodes individual movements
  $\Rightarrow$ computationally demanding, requires more data

- Lighthill-William-Richards (LWR), **macroscopic** traffic flow model
  $\Rightarrow$ vehicles treated as a continuous medium similar to particles in fluid
  $\Rightarrow$ one-dimensional (hyperbolic) conservation law

$$\begin{cases} \frac{\partial}{\partial t}\rho(t,x) + \frac{\partial}{\partial x} f(\rho(t,x)) = 0, & x \in \mathbb{R}, \quad t > 0, \\ \rho(0,x) = \bar{\rho}(x), & x \in \mathbb{R} \end{cases} \tag{6}$$

  $\Rightarrow$ faster implementation, less data-intensive
  $\Rightarrow$ overlooks traffic heterogeneity, oversimplifies traffic phenomena

Model-Based Approaches

- **Convergence analysis of FtL approximation scheme towards LWR model**[3]

[3] Holden and Risebro 2017.
[4] Di Francesco and Rosini 2015.

- **Convergence analysis of FtL approximation scheme towards LWR model**[3]
- Link between FtL and LWR based on atomization of initial density $\bar{\rho}$

$$\bar{x}_{i+1}^N := \sup\left\{x \in \mathbb{R} : \int_{\bar{x}_i^N}^{x} \bar{\rho}(y)dy = \frac{L}{N}\right\}, \quad i = 0, \cdots, N-1 \tag{7}$$

[3] Holden and Risebro 2017.
[4] Di Francesco and Rosini 2015.

- **Convergence analysis of FtL approximation scheme towards LWR model**[3]
- Link between FtL and LWR based on atomization of initial density $\bar{\rho}$

$$\bar{x}_{i+1}^N := \sup\left\{ x \in \mathbb{R} : \int_{\bar{x}_i^N}^{x} \bar{\rho}(y)dy = \frac{L}{N} \right\}, \quad i = 0, \cdots, N-1 \tag{7}$$

- Solution of PDE (5) can be recovered as many particle limit[4] of ODE system (6)

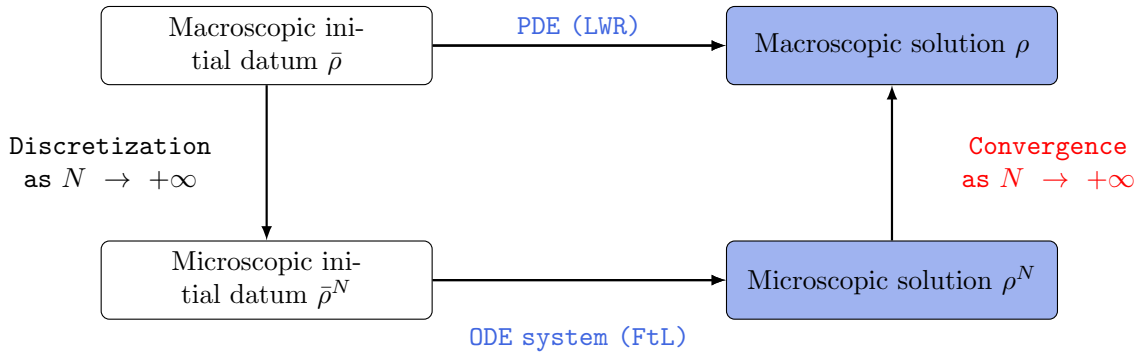

Coupled Resolution of a Microscopic ODE System and a Macroscopic PDE

[3] Holden and Risebro 2017.
[4] Di Francesco and Rosini 2015.

- Hybrid micro-macro models explored in traffic density reconstruction[5]

$$\begin{cases} \dot{x}_N^N(t) = v_{\max}, & t > 0, \\ \dot{x}_i^N(t) = v\left(\rho(t, x_i^N(t))\right), & t > 0, \quad i = 0, \cdots, N-1 \\ \frac{\partial}{\partial t}\rho(t,x) + \frac{\partial}{\partial x} f(\rho(t,x)) = \gamma^2 \frac{\partial^2}{\partial x^2}\rho(t,x), & x \in \mathbb{R}, \quad t > 0, \quad \gamma^6 > 0 \end{cases} \tag{8}$$

[5] Barreau, Aguiar, Liu, and Johansson 2021.

[6] $\gamma > 0$ is a diffusion correction parameter. Hopf proved that as γ tends to zero, the solution of LWR with diffusion term converges in the sense of distributions to the solution of classical LWR.

[7] Liu, Barreau, Cicic, and Johansson 2020.

Data-Driven Approaches

- Hybrid micro-macro models explored in traffic density reconstruction[5]

$$\begin{cases} \dot{x}_N^N(t) = v_{\max}, & t > 0, \\ \dot{x}_i^N(t) = v\left(\rho(t, x_i^N(t))\right), & t > 0, \quad i = 0, \cdots, N-1 \\ \frac{\partial}{\partial t}\rho(t,x) + \frac{\partial}{\partial x} f(\rho(t,x)) = \gamma^2 \frac{\partial^2}{\partial x^2}\rho(t,x), & x \in \mathbb{R}, \quad t > 0, \quad \gamma^6 > 0 \end{cases} \tag{8}$$

- **Partial state reconstruction**[7] using measurements from probe vehicles (PVs)
  $\Rightarrow$ low penetration rate $N_{\text{probes}} \ll N_{\text{total}}$
  $\Rightarrow$ recover density ρ from **limited** trajectories

[5] Barreau, Aguiar, Liu, and Johansson 2021.

[6] $\gamma > 0$ is a diffusion correction parameter. Hopf proved that as γ tends to zero, the solution of LWR with diffusion term converges in the sense of distributions to the solution of classical LWR.

[7] Liu, Barreau, Cicic, and Johansson 2020.

Data-Driven Approaches

- Hybrid micro-macro models explored in traffic density reconstruction[5]

$$\begin{cases} \dot{x}_N^N(t) = v_{\max}, & t > 0, \\ \dot{x}_i^N(t) = v\left(\rho(t, x_i^N(t))\right), & t > 0, \quad i = 0, \cdots, N-1 \\ \frac{\partial}{\partial t}\rho(t,x) + \frac{\partial}{\partial x} f(\rho(t,x)) = \gamma^2 \frac{\partial^2}{\partial x^2}\rho(t,x), & x \in \mathbb{R}, \quad t > 0, \quad \gamma^6 > 0 \end{cases} \tag{8}$$

- **Partial state reconstruction**[7] using measurements from probe vehicles (PVs)
  $\Rightarrow$ low penetration rate $N_{\text{probes}} \ll N_{\text{total}}$
  $\Rightarrow$ recover density ρ from **limited** trajectories
- Requires access to real-time positions, densities and instantaneous speeds of PVs

[5] Barreau, Aguiar, Liu, and Johansson 2021.

[6] $\gamma > 0$ is a diffusion correction parameter. Hopf proved that as γ tends to zero, the solution of LWR with diffusion term converges in the sense of distributions to the solution of classical LWR.

[7] Liu, Barreau, Cicic, and Johansson 2020.

Data-Driven Approaches

- Hybrid micro-macro models explored in traffic density reconstruction[5]

$$\begin{cases} \dot{x}_N^N(t) = v_{\max}, & t > 0, \\ \dot{x}_i^N(t) = v\left(\rho(t, x_i^N(t))\right), & t > 0, \quad i = 0, \cdots, N-1 \\ \frac{\partial}{\partial t}\rho(t,x) + \frac{\partial}{\partial x} f(\rho(t,x)) = \gamma^2 \frac{\partial^2}{\partial x^2}\rho(t,x), & x \in \mathbb{R}, \quad t > 0, \quad \gamma^6 > 0 \end{cases} \tag{8}$$

- **Partial state reconstruction**[7] using measurements from probe vehicles (PVs)
  $\Rightarrow$ low penetration rate $N_{\text{probes}} \ll N_{\text{total}}$
  $\Rightarrow$ recover density ρ from **limited** trajectories
- Requires access to real-time positions, densities and instantaneous speeds of PVs
- Prior approaches rely on knowledge of initial density $\bar{\rho}$
  $\Rightarrow$ **No access** to this critical information, need to leverage available data

[5] Barreau, Aguiar, Liu, and Johansson 2021.

[6] $\gamma > 0$ is a diffusion correction parameter. Hopf proved that as γ tends to zero, the solution of LWR with diffusion term converges in the sense of distributions to the solution of classical LWR.

[7] Liu, Barreau, Cicic, and Johansson 2020.

Table of Contents

Parametrized Microscopic Model

- **Limited data scenario** $\Rightarrow$ only **initial and final** $\left\{\left(\bar{x}^N, \bar{y}^N\right)\right\}_{i=0}^{n}$ positions of PVs

Parametrized Microscopic Model

- **Limited data scenario** $\Rightarrow$ only **initial and final** $\left\{\left(\bar{x}^N, \bar{y}^N\right)\right\}_{i=0}^{n}$ positions of PVs
- **Enhanced** version of FtL scheme (5) adding a parameter
  $\Rightarrow$ α^N accounts for unobserved vehicles between consecutive PVs
  $\Rightarrow$ bridges discrete (vehicle-level) dynamics to continuous (density-level) dynamics

Parametrized Microscopic Model

- **Limited data scenario** $\Rightarrow$ only **initial and final** $\left\{\left(\bar{x}^N, \bar{y}^N\right)\right\}_{i=0}^{n}$ positions of PVs
- **Enhanced** version of FtL scheme (5) adding a parameter
  $\Rightarrow$ α^N accounts for unobserved vehicles between consecutive PVs
  $\Rightarrow$ bridges discrete (vehicle-level) dynamics to continuous (density-level) dynamics
- Parametrized ODE system with finite time horizon

$$\begin{cases} \dot{x}_n^N(t) = v_{\max}, & t \in (0, T] \\ \dot{x}_i^N(t) = v\left(\rho_i^N(t)\right), & t \in (0, T] \quad i = 0, \cdots, n-1 \\ x_i^N(0) = \bar{x}_i^N, & i = 0, \cdots, n \end{cases} \tag{9}$$

  $\Rightarrow$ local discrete densities

$$\rho_i^N(t) := \frac{\alpha_i^N L}{N\left(x_{i+1}^N(t) - x_i^N(t)\right)}, \quad t \in (0, T], \quad i = 0, \cdots, n-1 \tag{10}$$

Parametrized Microscopic Model

- **Limited data scenario** $\Rightarrow$ only **initial and final** $\left\{\left(\bar{x}^N, \bar{y}^N\right)\right\}_{i=0}^{n}$ positions of PVs
- **Enhanced** version of FtL scheme (5) adding a parameter
  $\Rightarrow$ α^N accounts for unobserved vehicles between consecutive PVs
  $\Rightarrow$ bridges discrete (vehicle-level) dynamics to continuous (density-level) dynamics
- Parametrized ODE system with finite time horizon

$$\begin{cases} \dot{x}_n^N(t) = v_{\max}, & t \in (0, T] \\ \dot{x}_i^N(t) = v\left(\rho_i^N(t)\right), & t \in (0, T] \quad i = 0, \cdots, n-1 \\ x_i^N(0) = \bar{x}_i^N, & i = 0, \cdots, n \end{cases} \tag{9}$$

  $\Rightarrow$ local discrete densities

$$\rho_i^N(t) := \frac{\alpha_i^N L}{N\left(x_{i+1}^N(t) - x_i^N(t)\right)}, \quad t \in (0, T], \quad i = 0, \cdots, n-1 \tag{10}$$

- Piecewise constant Eulerian discrete density

$$\rho^N(t, x) := \sum_{i=0}^{N-1} \rho_i^N(t) \chi_{[x_i^N(t), x_{i+1}^N(t))}(x), \quad x \in \mathbb{R}, \quad t \in [0, T] \tag{11}$$

Well Posedness

- Assumptions on velocity

$$v \in C^1([0, +\infty)) \tag{12a}$$
$$v \text{ is decreasing on } [0, +\infty) \tag{12b}$$
$$v(0) = v_{\max} < \infty \tag{12c}$$

Well Posedness

- Assumptions on velocity

$$v \in C^1([0, +\infty)) \tag{12a}$$
$$v \text{ is decreasing on } [0, +\infty) \tag{12b}$$
$$v(0) = v_{\max} < \infty \tag{12c}$$

- Local existence and uniqueness of solution to (9) (for fixed α) via Picard-Lindelöf

Well Posedness

- Assumptions on velocity

$$v \in C^1([0, +\infty)) \tag{12a}$$
$$v \text{ is decreasing on } [0, +\infty) \tag{12b}$$
$$v(0) = v_{\max} < \infty \tag{12c}$$

- Local existence and uniqueness of solution to (9) (for fixed α) via Picard-Lindelöf
- Condition on initial car positions $\bar{x}_0^N < \bar{x}_1^N < \cdots < \bar{x}_{n-1}^N < \bar{x}_n^N$
  $\Rightarrow$ global existence

Lemma (Discrete maximum principle)

For solution $x(t)$ of (9) with v satisfying (12a)-(12c), for all $i = 0, \cdots, n-1$,

$$\frac{\alpha_i^N L}{NM} \leq x_{i+1}^N(t) - x_i^N(t) \leq \bar{x}_n^N - \bar{x}_0^N + (v_{\max} - v(M))\, t, \quad \forall t \in [0, T], \tag{13}$$

where $M := \max_i \left(\frac{\alpha_i^N L}{N(\bar{x}_{i+1}^N - \bar{x}_i^N)} \right)$

Sketch of proof

- Lower bound is satisfied at $t = 0$, aim at extending property for all times up to T

Sketch of proof

- Lower bound is satisfied at $t = 0$, aim at extending property for all times up to T
- Equivalent to show

$$\inf_{0<t\leq T} [x_{i+1}(t) - x_i(t)] \geq \frac{\alpha_i^N L}{NM}, \quad i = 0, \ldots, n-1. \tag{14}$$

$\Rightarrow$ **recursive argument** (backward from $n-1$ to 0)

Sketch of proof

- Lower bound is satisfied at $t = 0$, aim at extending property for all times up to T
- Equivalent to show

$$\inf_{0<t\leq T} [x_{i+1}(t) - x_i(t)] \geq \frac{\alpha_i^N L}{NM}, \quad i = 0, \dots, n-1. \tag{14}$$

  $\Rightarrow$ **recursive argument** (backward from $n-1$ to 0)
- Property is true for $i = n-1$

$$\begin{aligned} x_n(t) - x_{n-1}(t) =& \bar{x}_n - \bar{x}_{n-1} + \int_0^t \left(v_{\max} - v\left(\frac{\alpha_n^N L}{N(x_n(s) - x_{n-1}(s))} \right) \right) ds \\ \geq& \bar{x}_n - \bar{x}_{n-1} \geq \frac{\alpha_{n-1}^N L}{NM}. \end{aligned}$$

Sketch of proof

- Lower bound is satisfied at $t = 0$, aim at extending property for all times up to T
- Equivalent to show

$$\inf_{0<t\leq T} [x_{i+1}(t) - x_i(t)] \geq \frac{\alpha_i^N L}{NM}, \quad i = 0, \dots, n-1. \tag{14}$$

  $\Rightarrow$ **recursive argument** (backward from $n-1$ to 0)

- Property is true for $i = n-1$

$$\begin{aligned} x_n(t) - x_{n-1}(t) =& \bar{x}_n - \bar{x}_{n-1} + \int_0^t \left(v_{\max} - v\left(\frac{\alpha_n^N L}{N(x_n(s) - x_{n-1}(s))} \right) \right) ds \\ \geq& \bar{x}_n - \bar{x}_{n-1} \geq \frac{\alpha_{n-1}^N L}{NM}. \end{aligned}$$

- Assume property is verified for $j+1$ and prove it is still satisfied for j

$$\inf_{0<t\leq T} [x_{j+2}(t) - x_{j+1}(t)] \geq \frac{\alpha_{j+1}^N L}{NM}. \tag{15}$$

Sketch of proof

- By contradiction, assume that there exists $0 \leq t_1 < t_2$ such that

$$\begin{cases} x_{j+1}(t) - x_j(t) \geq \frac{\alpha_j^N L}{NM}, & t < t_1 \\ x_{j+1}(t) - x_j(t) = \frac{\alpha_j^N L}{NM}, & t = t_1 \\ x_{j+1}(t) - x_j(t) < \frac{\alpha_j^N L}{NM}, & t_1 < t \leq t_2. \end{cases} \tag{16}$$

Sketch of proof

- By contradiction, assume that there exists $0 \leq t_1 < t_2$ such that

$$\begin{cases} x_{j+1}(t) - x_j(t) \geq \frac{\alpha_j^N L}{NM}, & t < t_1 \\ x_{j+1}(t) - x_j(t) = \frac{\alpha_j^N L}{NM}, & t = t_1 \\ x_{j+1}(t) - x_j(t) < \frac{\alpha_j^N L}{NM}, & t_1 < t \leq t_2. \end{cases} \tag{16}$$

- Since v is decreasing

$$\begin{aligned} x_j(t) =& x_j(t_1) + \int_{t_1}^{t} v\left(\frac{\alpha_j^N L}{N(x_{j+1}(s) - x_j(s))}\right) ds \\ \leq& x_j(t_1) + v(M)(t - t_1), \end{aligned}$$

- Moreover from (15), for $t_1 < t \leq t_2$,

$$\begin{aligned} x_{j+1}(t) =& x_{j+1}(t_1) + \int_{t_1}^{t} v\left(\frac{\alpha_{j+1}^N L}{N(x_{j+2}(s) - x_{j+1}(s))}\right) ds \\ \geq& x_{j+1}(t_1) + v(M)(t - t_1) \end{aligned}$$

$$\Rightarrow x_{j+1}(t) - x_j(t) \geq x_{j+1}(t_1) - x_j(t_1) = \frac{\alpha_j^N L}{NM}$$

which contradicts (16), so that (14) is satisfied.

Sketch of proof

- Show upper bound for $i = 0, \dots, n-1$ and $t \in [0, T]$
- Recalling assumptions on v and applying system's dynamics

$$
\begin{aligned}
x_{i+1}(t) - x_i(t) &= x_{i+1}(0) - x_i(0) + \int_0^t (\dot{x}_{i+1}(s) - \dot{x}_i(s))\, ds \\
&\leq \bar{x}_{i+1} - \bar{x}_i + \int_0^t \left(v_{\max} - v\left(\frac{\alpha_i^N L}{N(x_{i+1}(s) - x_i(s))} \right) \right) ds \\
&\leq \bar{x}_n - \bar{x}_0 + \left(v_{\max} - v(M)\right) t,
\end{aligned}
$$

- Last equality is obtained from lower bound $\Rightarrow$ proof is complete

ODE-Constrained Optimization

- Physical conditions on $\alpha := \alpha^N$ induce feasible set

$$\mathcal{A}_N := \left\{ \alpha \in \mathbb{R}^n : \quad \alpha_i \in \left[1, \bar{z}_i^N\right], \quad i = 0, \dots, n-1, \quad \sum_{i=0}^{n-1} \alpha_i = N \right\} \tag{17}$$

with $\bar{z}_i^N := \min \left\{ \frac{N\left(\bar{x}_{i+1}^N - \bar{x}_i^N\right)}{L}, \frac{N\left(\bar{y}_{i+1}^N - \bar{y}_i^N\right)}{L} \right\}, \quad i = 0, \dots, n-1$

[8] Baloul, Hayat, Liard, and Lissy 2025.

ODE-Constrained Optimization

- Physical conditions on $\alpha := \alpha^N$ induce feasible set

$$\mathcal{A}_N := \left\{ \alpha \in \mathbb{R}^n : \quad \alpha_i \in \left[1, \bar{z}_i^N\right], \quad i = 0, \dots, n-1, \quad \sum_{i=0}^{n-1} \alpha_i = N \right\} \tag{17}$$

with $\bar{z}_i^N := \min\left\{ \frac{N\left(\bar{x}_{i+1}^N - \bar{x}_i^N\right)}{L}, \frac{N\left(\bar{y}_{i+1}^N - \bar{y}_i^N\right)}{L} \right\}, \quad i = 0, \dots, n-1$

- **Approximate density reconstruction**[8] $\Rightarrow$ find optimal interaction parameter α

$$\begin{aligned} \underset{\alpha}{\text{minimize}} \quad & \frac{1}{2} \left\| x(T) - \bar{y} \right\|^2 \\ \text{s.t.} \quad & \dot{x}(t) = V\left(W_\alpha x(t) + b_\alpha(t)\right) \\ & x(0) = \bar{x} \\ & \alpha \in \mathcal{A}_N \end{aligned} \tag{18}$$

[8] Baloul, Hayat, Liard, and Lissy 2025.

ODE-Constrained Optimization

- Physical conditions on $\alpha := \alpha^N$ induce feasible set

$$\mathcal{A}_N := \left\{ \alpha \in \mathbb{R}^n : \quad \alpha_i \in \left[1, \bar{z}_i^N\right], \quad i = 0, \dots, n-1, \quad \sum_{i=0}^{n-1} \alpha_i = N \right\} \tag{17}$$

with $\bar{z}_i^N := \min\left\{ \frac{N\left(\bar{x}_{i+1}^N - \bar{x}_i^N\right)}{L}, \frac{N\left(\bar{y}_{i+1}^N - \bar{y}_i^N\right)}{L} \right\}, \quad i = 0, \dots, n-1$

- **Approximate density reconstruction**[8] $\Rightarrow$ find optimal interaction parameter α

$$\begin{aligned} \underset{\alpha}{\text{minimize}} \quad & \frac{1}{2} \left\| x(T) - \bar{y} \right\|^2 \\ \text{s.t.} \quad & \dot{x}(t) = V\left(W_\alpha x(t) + b_\alpha(t)\right) \\ & x(0) = \bar{x} \\ & \alpha \in \mathcal{A}_N \end{aligned} \tag{18}$$

- Existence of solutions guaranteed by assumptions on $V := v \circ \frac{1}{\cdot}$ (continuity of v) and constraints on α (compactness of $\mathcal{A}_N$)

[8] Baloul, Hayat, Liard, and Lissy 2025.

ODE-Constrained Optimization

- Physical conditions on $\alpha := \alpha^N$ induce feasible set

$$\mathcal{A}_N := \left\{ \alpha \in \mathbb{R}^n : \quad \alpha_i \in \left[1, \bar{z}_i^N\right], \quad i = 0, \dots, n-1, \quad \sum_{i=0}^{n-1} \alpha_i = N \right\} \tag{17}$$

with $\bar{z}_i^N := \min \left\{ \frac{N\left(\bar{x}_{i+1}^N - \bar{x}_i^N\right)}{L}, \frac{N\left(\bar{y}_{i+1}^N - \bar{y}_i^N\right)}{L} \right\}, \quad i = 0, \dots, n-1$

- **Approximate density reconstruction**[8] $\Rightarrow$ find optimal interaction parameter α

$$\begin{aligned} \underset{\alpha}{\text{minimize}} \quad & \frac{1}{2} \left\| x(T) - \bar{y} \right\|^2 \\ \text{s.t.} \quad & \dot{x}(t) = V\left(W_\alpha x(t) + b_\alpha(t)\right) \\ & x(0) = \bar{x} \\ & \alpha \in \mathcal{A}_N \end{aligned} \tag{18}$$

- Existence of solutions guaranteed by assumptions on $V := v \circ \frac{1}{\cdot}$ (continuity of v) and constraints on α (compactness of $\mathcal{A}_N$)
- No uniqueness (a priori) since nonlinear dynamics can lead to multiple minima

[8] Baloul, Hayat, Liard, and Lissy 2025.

Learning Method

- Dataset consists of **artificial data** based on simulated (classical) FtL dynamics (5)
- Sampling of PVs yielding a **balanced representation** of overall traffic

Learning Method

- Dataset consists of **artificial data** based on simulated (classical) FtL dynamics (5)
- Sampling of PVs yielding a **balanced representation** of overall traffic
- Neural network architecture designed to **understand dynamics of traffic**

Learning Method

- Dataset consists of **artificial data** based on simulated (classical) FtL dynamics (5)
- Sampling of PVs yielding a **balanced representation** of overall traffic
- Neural network architecture designed to **understand dynamics of traffic**
- Residual network (ResNet) where each block corresponds to a single time step
- Input $\bar{x}$ and state $x(.)$ is propagated by mirroring Euler discretization

$$x(t + \Delta t) = x(t) + V(Wx(t) + b)\Delta t \tag{19}$$

- Weights and biases W, b are functions of α

$$\begin{cases} W_{i,i} & := -\frac{N}{\alpha_i L}, i = 0, \ldots, n-1, \\ W_{i,i+1} & := \frac{N}{\alpha_i L}, i = 1, \ldots, n-2, \\ W_{i,j} & := 0, \text{otherwise}, \end{cases} \tag{20}$$

$$b_i(t) =:= \delta_{i,n} \frac{N}{\alpha_{n-1} L} \left(v_{\max} t + \bar{x}_n^N \right), \quad t \in [0, T] \tag{21}$$

- Nonlinear dynamic map V acts as physics grounded activation function
- Backpropagation to minimize predictions errors $\frac{1}{n} \sum_{j=0}^{n} |x_j^\alpha(T) - \bar{y}_j^N|^2$

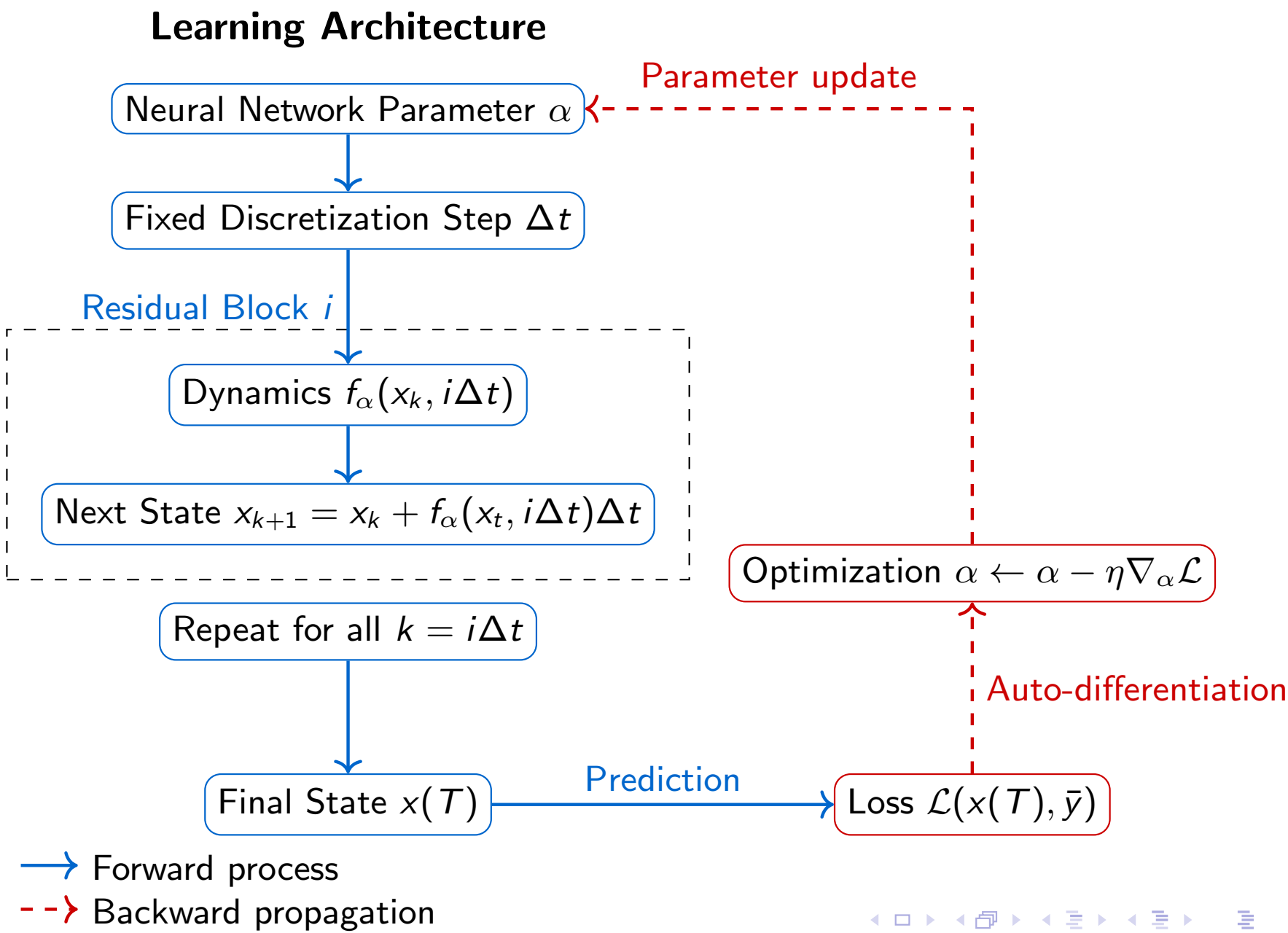
Learning Architecture
Parameter update
Neural Network Parameter α
Fixed Discretization Step Δt
Residual Block i
Dynamics $f_\alpha(x_k, i\Delta t)$
Next State $x_{k+1} = x_k + f_\alpha(x_t, i\Delta t)\Delta t$
Optimization $\alpha \leftarrow \alpha - \eta \nabla_\alpha \mathcal{L}$
Repeat for all $k = i\Delta t$
Auto-differentiation
Final State $x(T)$
Prediction
Loss $\mathcal{L}(x(T), \bar{y})$
Forward process
Backward propagation

Model validation

- Through predicted parameter $\bar{\alpha}$, training yields piecewise constant discrete density

$$\rho^N(t,x) = \sum_{i=0}^{n-1} \frac{\bar{\alpha}_i L}{N(x_{i+1}^N(t) - x_i^N(t))} \chi_{[x_i^N(t), x_{i+1}^N(t))}(x), \quad x \in \mathbb{R}, \quad t \in [0,T], \qquad (22)$$

Model validation

- Through predicted parameter $\bar{\alpha}$, training yields piecewise constant discrete density

$$\rho^N(t,x) = \sum_{i=0}^{n-1} \frac{\bar{\alpha}_i L}{N(x_{i+1}^N(t) - x_i^N(t))} \chi_{[x_i^N(t), x_{i+1}^N(t))}(x), \quad x \in \mathbb{R}, \quad t \in [0,T], \tag{22}$$

- Simulation on **test data** by solving ODE system

$$\begin{cases} \dot{x}_i^N(t) = v\left(\rho^N(t, x_i(t)^+)\right), & t \in (0,T], \\ x_i^N(0) = \bar{x}_i^N & i = 0, \ldots, n_{\text{test}} \end{cases} \tag{23}$$

Model validation

- Through predicted parameter $\bar{\alpha}$, training yields piecewise constant discrete density

$$\rho^N(t,x) = \sum_{i=0}^{n-1} \frac{\bar{\alpha}_i L}{N(x_{i+1}^N(t) - x_i^N(t))} \chi_{[x_i^N(t), x_{i+1}^N(t))}(x), \quad x \in \mathbb{R}, \quad t \in [0,T], \tag{22}$$

- Simulation on **test data** by solving ODE system

$$\begin{cases} \dot{x}_i^N(t) = v\left(\rho^N(t, x_i(t)^+)\right), & t \in (0,T], \\ x_i^N(0) = \bar{x}_i^N & i = 0, \ldots, n_{\text{test}} \end{cases} \tag{23}$$

- Assess model's performance by measuring test error $\frac{1}{n_{\text{test}}} \sum_{j=0}^{n_{\text{test}}} |x_j(T) - \bar{y}_i^N|^2$

Scheme of Model

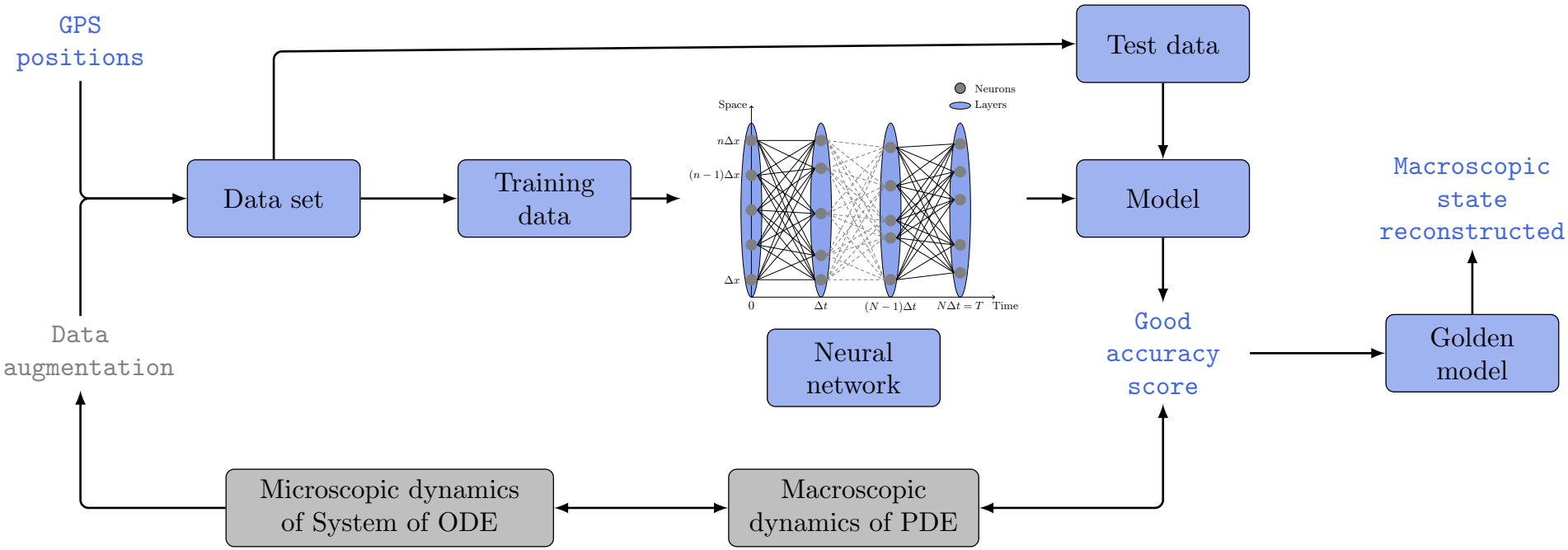

Traffic Flow Reconstruction Pipeline

Table of Contents

Outline of Convergence Analysis

- Prove that, **if only using data from dynamical systems**, approximate density ρ^N predicted by our machine learning model converges to solution of the LWR model (6) when the number of vehicles approaches infinity

Outline of Convergence Analysis

- Prove that, **if only using data from dynamical systems**, approximate density ρ^N predicted by our machine learning model converges to solution of the LWR model (6) when the number of vehicles approaches infinity
- Main challenge lies in imposing a condition on distribution of α which would guarantee convergence

Outline of Convergence Analysis

- Prove that, **if only using data from dynamical systems**, approximate density ρ^N predicted by our machine learning model converges to solution of the LWR model (6) when the number of vehicles approaches infinity
- Main challenge lies in imposing a condition on distribution of α which would guarantee convergence
- Demonstrate that discrete initial density $\rho^N(0, \cdot)$ converges to the initial condition $\bar{\rho}$ in the LWR model (6) under this additional assumption

Outline of Convergence Analysis

- Prove that, **if only using data from dynamical systems**, approximate density ρ^N predicted by our machine learning model converges to solution of the LWR model (6) when the number of vehicles approaches infinity
- Main challenge lies in imposing a condition on distribution of α which would guarantee convergence
- Demonstrate that discrete initial density $\rho^N(0,\cdot)$ converges to the initial condition $\bar{\rho}$ in the LWR model (6) under this additional assumption
- In addition to Euler discrete density (11), consider empirical discrete density

$$\widehat{\rho}^N(t,\cdot) \coloneqq \frac{L}{N}\sum_{i=0}^{n-1}\alpha_i^N \delta_{x_i(t)}(\cdot), \quad t \in [0,T]. \tag{24}$$

Outline of Convergence Analysis

- Prove that, **if only using data from dynamical systems**, approximate density ρ^N predicted by our machine learning model converges to solution of the LWR model (6) when the number of vehicles approaches infinity
- Main challenge lies in imposing a condition on distribution of α which would guarantee convergence
- Demonstrate that discrete initial density $\rho^N(0,\cdot)$ converges to the initial condition $\bar{\rho}$ in the LWR model (6) under this additional assumption
- In addition to Euler discrete density (11), consider empirical discrete density

$$\widehat{\rho}^N(t,\cdot) := \frac{L}{N}\sum_{i=0}^{n-1}\alpha_i^N\delta_{x_i(t)}(\cdot), \quad t\in[0,T]. \tag{24}$$

- **Important observation**: by construction, initial traffic density must satisfy

$$\bar{x}_{i+1} = \sup\left\{x\in\mathbb{R} : \int_{\bar{x}_i}^{x}\bar{\rho}(y)dy \le \frac{\alpha_i L}{N}\right\}, \quad i=0,\dots,n-1 \tag{25}$$

$\Rightarrow$ although no access to ground-truth initial car density $\bar{\rho}$, initial positions $\bar{x}_i$ of probe vehicles verify (25) (i.e. number of unobserved vehicles between $[x_i, x_{i+1})$ is given by α_i)

Convergence Result

- Weak solution of (6) is entropy admissible if it satisfies **Kruzhkov entropy condition**

$$\int_0^T \int_{\mathbb{R}} |u-k| \frac{\partial \phi}{\partial t} + \operatorname{sign}(u-k)(f(u)-f(k)) \frac{\partial \phi}{\partial x} dx dt \geq 0, \quad \forall k \in \mathbb{R} \tag{26}$$

Theorem Convergence of approximate density to solution of LWR

Under some assumptions, piecewise-constant density

$$\rho^N(t,x) = \sum_{i=0}^{n-1} \frac{\bar{\alpha}_i^N L}{N(x_{i+1}^N(t) - x_i^N(t))} \chi_{[x_i^N(t), x_{i+1}^N(t))}(x), \quad x \in \mathbb{R}, \quad t \in [0,T], \tag{27}$$

where $\bar{\alpha}_i^N \in \mathcal{A}_N$ is a solution to (18) converges to **unique entropy** solution ρ of

$$\begin{aligned} &\frac{\partial \rho}{\partial t}(t,x) + \frac{\partial f(\rho)}{\partial x}(t,x) = 0, \quad x \in \mathbb{R}, \quad t \in [0,T], \\ &\rho(0,x) = \bar{\rho}(x), \quad x \in \mathbb{R} \end{aligned} \tag{28}$$

Convergence Result

- Weak solution of (6) is entropy admissible if it satisfies **Kruzhkov entropy condition**

$$\int_0^T \int_{\mathbb{R}} |u-k| \frac{\partial \phi}{\partial t} + \operatorname{sign}(u-k)(f(u)-f(k)) \frac{\partial \phi}{\partial x} dx dt \geq 0, \quad \forall k \in \mathbb{R} \tag{26}$$

Theorem Convergence of approximate density to solution of LWR

Under some assumptions, piecewise-constant density

$$\rho^N(t,x) = \sum_{i=0}^{n-1} \frac{\bar{\alpha}_i^N L}{N(x_{i+1}^N(t) - x_i^N(t))} \chi_{[x_i^N(t), x_{i+1}^N(t))}(x), \quad x \in \mathbb{R}, \quad t \in [0,T], \tag{27}$$

where $\bar{\alpha}_i^N \in \mathcal{A}_N$ is a solution to (18) converges to **unique entropy** solution ρ of

$$\begin{aligned} &\frac{\partial \rho}{\partial t}(t,x) + \frac{\partial f(\rho)}{\partial x}(t,x) = 0, \quad x \in \mathbb{R}, \quad t \in [0,T], \\ &\rho(0,x) = \bar{\rho}(x), \quad x \in \mathbb{R} \end{aligned} \tag{28}$$

- Impose a condition that ensures controlled growth of α_N

Sketch of proof

- Ensures discretization aligns consistently with true initial density when $N \to \infty$
- Notations: for $t \in [0, T]$, $\rho(t) := \rho(t, \cdot)$ and $\widehat{\rho}(t) := \widehat{\rho}(t, \cdot)$.
  In particular, at $t = 0$, $\rho(0) := \rho(0, \cdot)$ and $\widehat{\rho}(0) := \widehat{\rho}(0, \cdot)$

Sketch of proof

- Ensures discretization aligns consistently with true initial density when $N \to \infty$
- Notations: for $t \in [0, T]$, $\rho(t) := \rho(t, \cdot)$ and $\widehat{\rho}(t) := \widehat{\rho}(t, \cdot)$.
  In particular, at $t = 0$, $\rho(0) := \rho(0, \cdot)$ and $\widehat{\rho}(0) := \widehat{\rho}(0, \cdot)$
- Use **Wasserstein distance** defined in Di Francesco and Rosini 2015 by

$$\mathrm{W}_{L,1}(f, g) = \|f(]-\infty, \cdot]) - g(]-\infty, \cdot]\|_{L^1(\mathbb{R},\mathbb{R})} \tag{29}$$

Proposition

Let $\bar{\rho}$ satisfy (25) and assume that

$$\max_{i=0,\dots,n-1} \alpha_i^N = o(N) \tag{30}$$

Then, both sequences $(\rho^N(0))_{n\in\mathbb{N}}$ and $(\widehat{\rho}^N(0))_{n\in\mathbb{N}}$ converge to $\bar{\rho}$ in the sense of the $\mathrm{W}_{L,1}$ -Wasserstein distance in (29)

Remark

A particular case of assumption (30) is when $\max_{i=0,\dots,n-1} \alpha_i^N \leq \frac{CN}{\log(N)}$ for some $C > 0$

Sketch of proof

- Using $l_N := L/N$, $\mathrm{W}_{L,1}$- distance and discrete density in (10)

$$\begin{aligned}\mathrm{W}_{L,1}(\rho^N(0), \widehat{\rho}^N(0)) &= \sum_{i=0}^{n-1} \int_{\bar{x}_i}^{\bar{x}_{i+1}^N} \left(\alpha_i^N l_N - \rho_i^N(t)\,(x - \bar{x}_i)\right) dx \\ &= \sum_{i=0}^{n-1} \alpha_i^N l_N \int_{\bar{x}_i}^{\bar{x}_{i+1}} \left(1 - \frac{x - \bar{x}_i}{\bar{x}_{i+1} - \bar{x}_i}\right) dx \\ &\leq \max_{i=0,\dots,n} \{\alpha_i^N\} l_N\,(\bar{x}_n - \bar{x}_0)\end{aligned} \tag{31}$$

$\Rightarrow$ it suffices to prove that $(\widehat{\rho}^N(0))_{n\in\mathbb{N}}$ converges to $\bar{\rho}$ wrt $\mathrm{W}_{L,1}$- distance

Sketch of proof

- Using $l_N := L/N$, $\mathrm{W}_{L,1}$- distance and discrete density in (10)

$$\begin{aligned}\mathrm{W}_{L,1}(\rho^N(0), \widehat{\rho}^N(0)) &= \sum_{i=0}^{n-1} \int_{\bar{x}_i}^{\bar{x}_{i+1}^N} \left(\alpha_i^N l_N - \rho_i^N(t)\,(x - \bar{x}_i)\right) dx \\ &= \sum_{i=0}^{n-1} \alpha_i^N l_N \int_{\bar{x}_i}^{\bar{x}_{i+1}} \left(1 - \frac{x - \bar{x}_i}{\bar{x}_{i+1} - \bar{x}_i}\right) dx \\ &\leq \max_{i=0,\dots,n} \{\alpha_i^N\} l_N\,(\bar{x}_n - \bar{x}_0)\end{aligned} \tag{31}$$

  $\Rightarrow$ it suffices to prove that $(\widehat{\rho}^N(0))_{n\in\mathbb{N}}$ converges to $\bar{\rho}$ wrt $\mathrm{W}_{L,1}$- distance

- Using expressions of both Euler (11) and empirical (24) discrete densities

$$\begin{aligned}&\mathrm{W}_{L,1}(\widehat{\rho}^N(0), \bar{\rho}) \\ &= \sum_{i=0}^{n-2} \int_{\bar{x}_i}^{\bar{x}_{i+1}} \left(\sum_{j=0}^{i} \alpha_j^N l_N - \int_{-\infty}^{x} \bar{\rho}(y)dy\right) dx + \int_{\bar{x}_{n-1}}^{\bar{x}_n} \left(L - \int_{-\infty}^{x} \bar{\rho}(y)dy\right) dx \\ &= \sum_{i=0}^{n-2} \int_{\bar{x}_i}^{\bar{x}_{i+1}} \left(\left(\sum_{j=0}^{i-1} \alpha_j^N l_N - \int_{\bar{x}_0}^{\bar{x}_i} \bar{\rho}(y)dy\right) + \left(\alpha_i^N l_N - \int_{\bar{x}_i}^{x} \bar{\rho}(y)dy\right)\right) dx \\ &\quad + \int_{\bar{x}_{n-1}}^{\bar{x}_n} \left(\sum_{j=0}^{n-2} \alpha_j^N l_N - \int_{\bar{x}_0}^{\bar{x}_{n-1}} \bar{\rho}(y)dy\right) + \left(\alpha_{n-1}^N l_N - \int_{\bar{x}_{n-1}}^{x} \bar{\rho}(y)dy\right) dx\end{aligned}$$

Sketch of proof

- From atomization of initial density (25), deduce

$$
\begin{aligned}
&\mathrm{W}_{L,1}(\widehat{\rho}^N(0), \bar{\rho}) \\
&\leq \sum_{i=0}^{n-2} \int_{\bar{x}_i}^{\bar{x}_{i+1}} \left(\alpha_i^N l_N - \int_{\bar{x}_i}^{x} \bar{\rho}(y)dy \right) dx + \int_{\bar{x}_{n-1}}^{\bar{x}_n} \left(\alpha_{n-1}^N l_N - \int_{\bar{x}_{n-1}}^{x} \bar{\rho}(y)dy \right) dx \\
&= \sum_{i=0}^{n-1} \alpha_i^N l_N \int_{\bar{x}_i}^{\bar{x}_{i+1}} \left(1 - \frac{1}{\alpha_i^N l_N} \int_{\bar{x}_i}^{x} \bar{\rho}(y)dy \right) dx \\
&\leq \max_{i=0,\ldots,n} \left\{ \alpha_i^N \right\} l_N (\bar{x}_n - \bar{x}_0)
\end{aligned}
$$

Sketch of proof

- From atomization of initial density (25), deduce

$$
\begin{aligned}
&\mathrm{W}_{L,1}(\widehat{\rho}^N(0), \bar{\rho}) \\
&\leq \sum_{i=0}^{n-2} \int_{\bar{x}_i}^{\bar{x}_{i+1}} \left(\alpha_i^N l_N - \int_{\bar{x}_i}^{x} \bar{\rho}(y)dy \right) dx + \int_{\bar{x}_{n-1}}^{\bar{x}_n} \left(\alpha_{n-1}^N l_N - \int_{\bar{x}_{n-1}}^{x} \bar{\rho}(y)dy \right) dx \\
&= \sum_{i=0}^{n-1} \alpha_i^N l_N \int_{\bar{x}_i}^{\bar{x}_{i+1}} \left(1 - \frac{1}{\alpha_i^N l_N} \int_{\bar{x}_i}^{x} \bar{\rho}(y)dy \right) dx \\
&\leq \max_{i=0,\dots,n} \left\{ \alpha_i^N \right\} l_N(\bar{x}_n - \bar{x}_0)
\end{aligned}
$$

- From assumption (30) and estimate (31), conclude that $(\rho^N(0))_{n\in\mathbb{N}}$ converges to $\bar{\rho}$ in sense of $\mathrm{W}_{L,1}$-Wasserstein distance

Sketch of proof

- From atomization of initial density (25), deduce

$$
\begin{aligned}
&\mathrm{W}_{L,1}(\widehat{\rho}^N(0), \bar{\rho}) \\
&\leq \sum_{i=0}^{n-2} \int_{\bar{x}_i}^{\bar{x}_{i+1}} \left(\alpha_i^N l_N - \int_{\bar{x}_i}^{x} \bar{\rho}(y)dy \right) dx + \int_{\bar{x}_{n-1}}^{\bar{x}_n} \left(\alpha_{n-1}^N l_N - \int_{\bar{x}_{n-1}}^{x} \bar{\rho}(y)dy \right) dx \\
&= \sum_{i=0}^{n-1} \alpha_i^N l_N \int_{\bar{x}_i}^{\bar{x}_{i+1}} \left(1 - \frac{1}{\alpha_i^N l_N} \int_{\bar{x}_i}^{x} \bar{\rho}(y)dy \right) dx \\
&\leq \max_{i=0,\dots,n} \left\{ \alpha_i^N \right\} l_N(\bar{x}_n - \bar{x}_0)
\end{aligned}
$$

- From assumption (30) and estimate (31), conclude that $(\rho^N(0))_{n\in\mathbb{N}}$ converges to $\bar{\rho}$ in sense of $\mathrm{W}_{L,1}$-Wasserstein distance
- Moreover, by leveraging expression of discrete density (11), generalize convergence to unique entropy solution of conservation law (6), referring to Di Francesco and Rosini 2015, Theorem 3 $\Rightarrow$ require only minor modifications to original arguments

Table of Contents

Numerical experiments

- Parameters
  - Maximum traffic speed $v_{\max} = 120$ km/h
  - Maximum traffic density $\rho_{\max} = 200$ cars/km
  - Greenshields velocity $v(\rho) = v_{\max} \max\left\{1 - \frac{\rho}{\rho_{max}}, 0\right\}, \quad \rho \in [0, \rho_{max}]$
  - Final time horizon $T = 0.1$ h or $T = 0.2$
- Sampling such 10% **of total fleet serve as PVs for training and** 2.5% **for testing**

Numerical experiments

- Parameters
  - Maximum traffic speed $v_{\max} = 120$ km/h
  - Maximum traffic density $\rho_{\max} = 200$ cars/km
  - Greenshields velocity $v(\rho) = v_{\max} \max\left\{1 - \frac{\rho}{\rho_{max}}, 0\right\}, \quad \rho \in [0, \rho_{max}]$
  - Final time horizon $T = 0.1$ h or $T = 0.2$
- Sampling such 10% **of total fleet serve as PVs for training and** 2.5% **for testing**
- Two traffic scenarii modelled
  1. Shock wave represents an abrupt transition in traffic conditions
  2. Stop-and-go wave characterized by alternating regions of congestion and free flow

Shock wave scenario

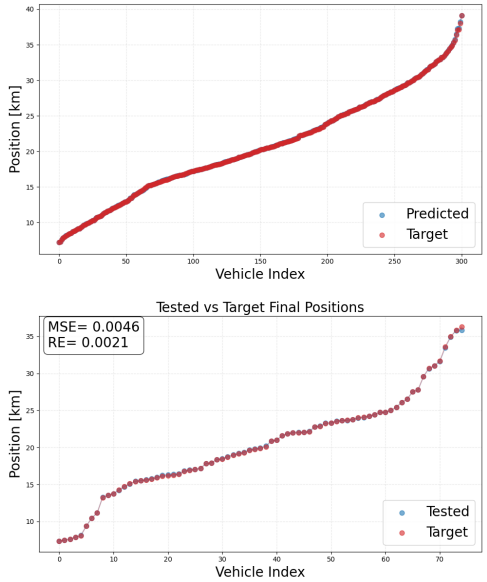

(a) $N = 3000$

Comparison of predicted and target final PV positions
Top Results from **training** procedure
Bottom Results on **test** sounds

Shock wave scenario

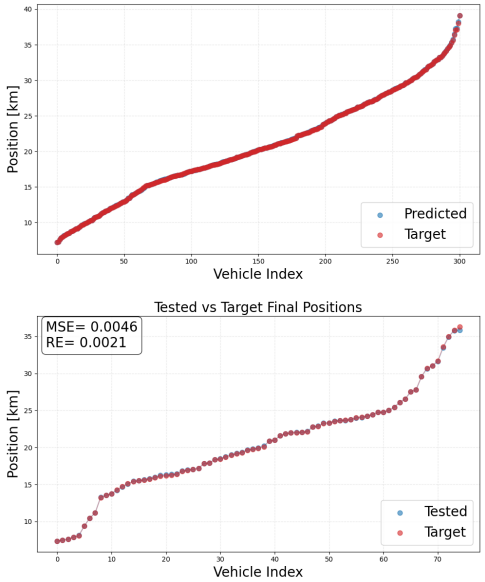

(a) $N = 3000$

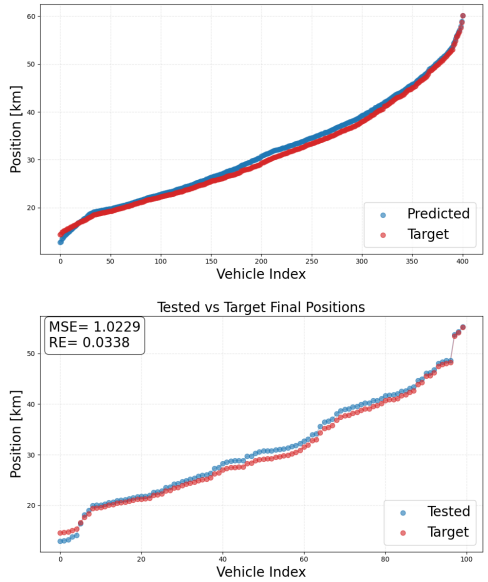

(b) $N = 4000$

Comparison of predicted and target final PV positions
Top Results from **training** procedure
Bottom Results on **test** sounds

Shock wave scenario

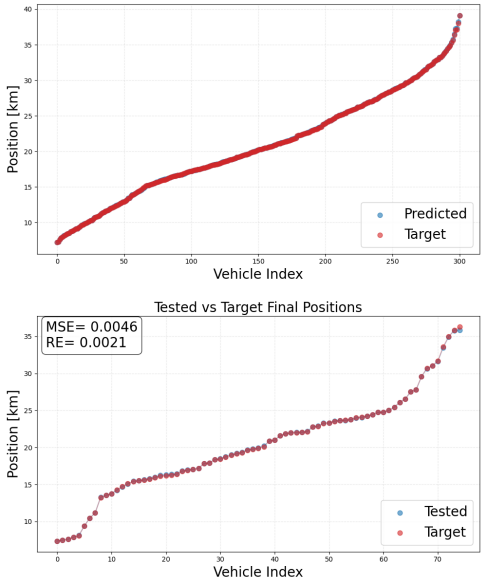

(a) $N = 3000$

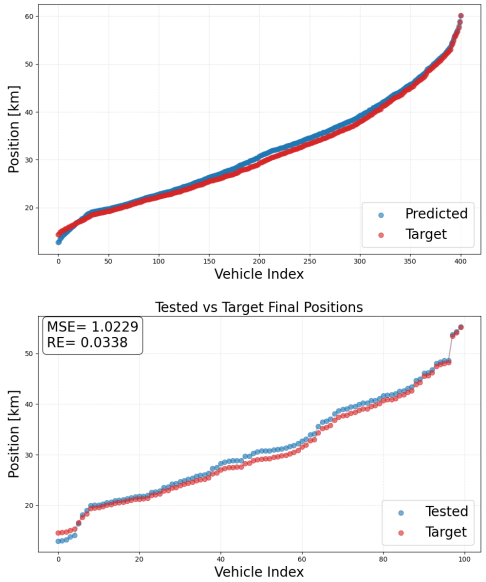

(b) $N = 4000$

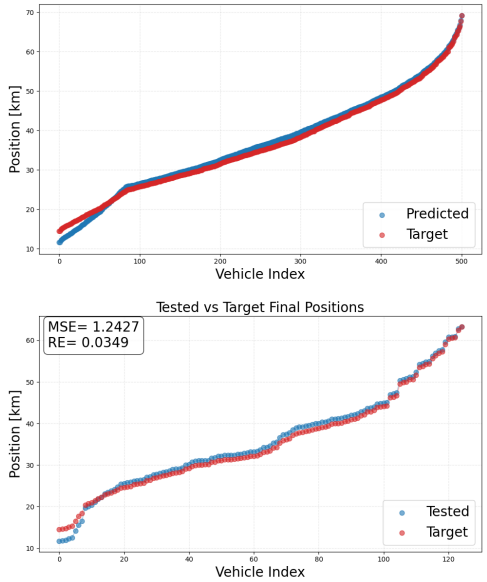

(c) $N = 5000$

Comparison of predicted and target final PV positions
Top Results from **training** procedure
Bottom Results on **test** sounds

Shock wave scenario

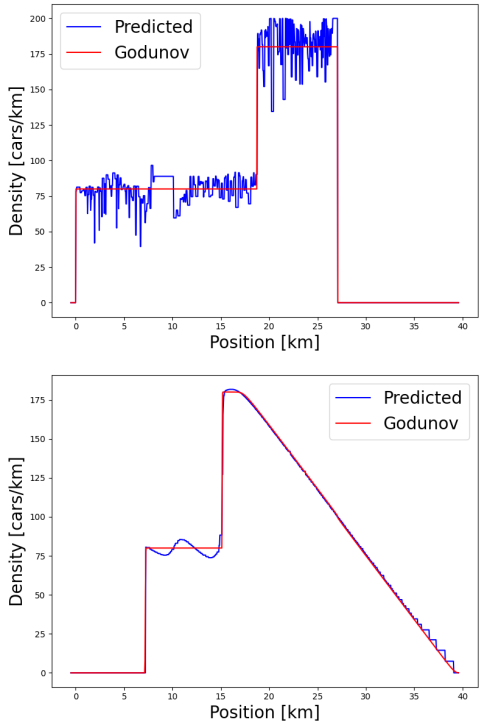

(a) $N = 3000$

Comparison of reconstructed and macroscopic densities
Top Initial densities
Bottom Final densities

Shock wave scenario

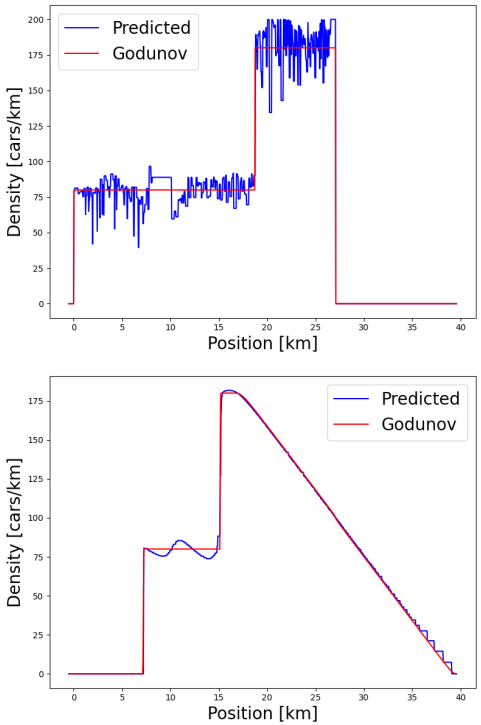

(a) $N = 3000$

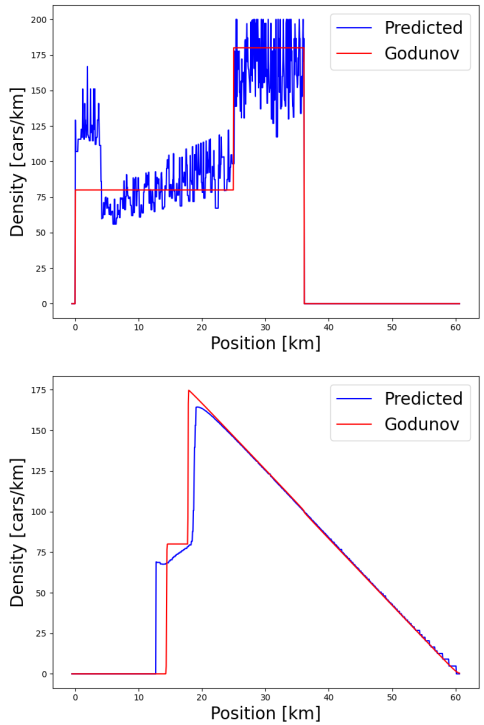

(b) $N = 4000$

Comparison of reconstructed and macroscopic densities
Top Initial densities
Bottom Final densities

Shock wave scenario

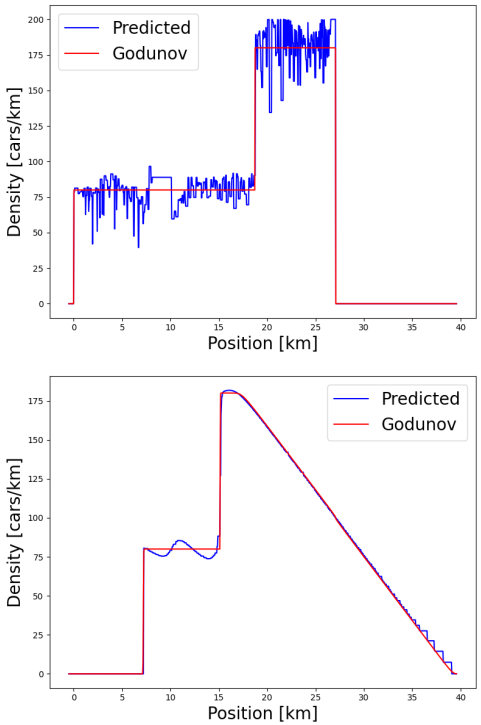

(a) $N = 3000$

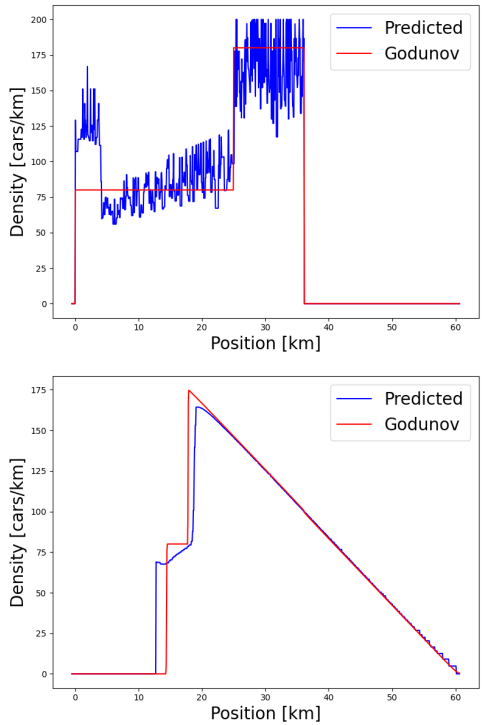

(b) $N = 4000$

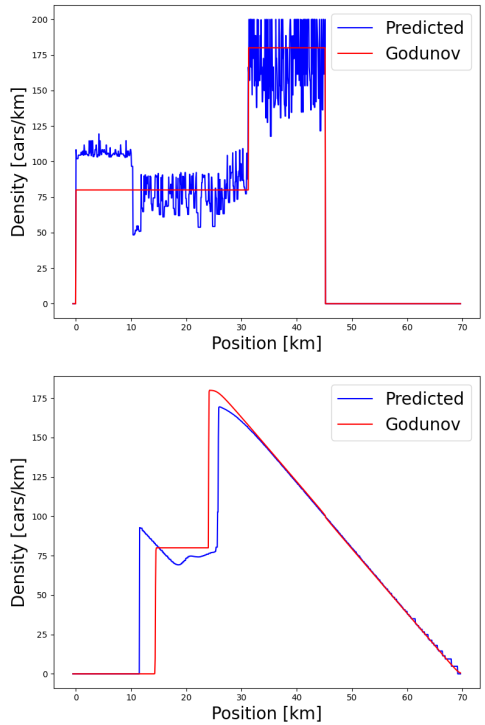

(c) $N = 5000$

Comparison of reconstructed and macroscopic densities
Top Initial densities
Bottom Final densities

Shock wave scenario

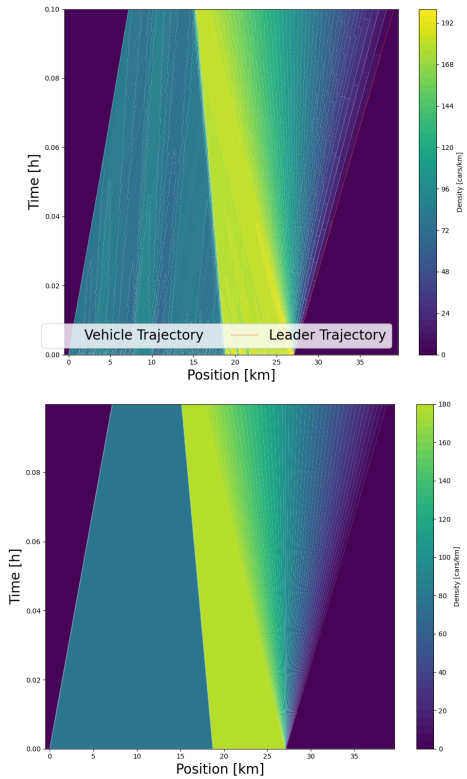

(a) $N = 3000$

Comparison of **reconstructed** and **macroscopic** densities
Top Reconstructed density from learning-based optimization
Bottom Macroscopic density from LWR PDE (Godunov scheme)

Shock wave scenario

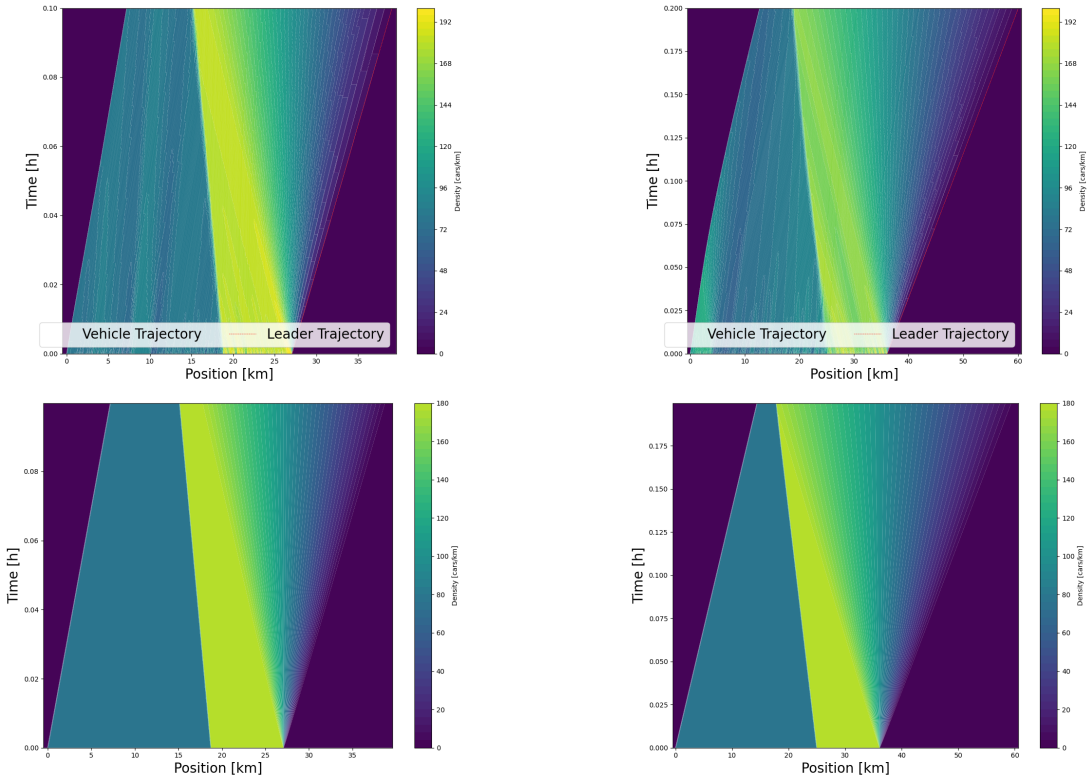

(a) $N = 3000$ (b) $N = 4000$

Comparison of **reconstructed** and **macroscopic** densities
Top Reconstructed density from learning-based optimization
Bottom Macroscopic density from LWR PDE (Godunov scheme)

Shock wave scenario

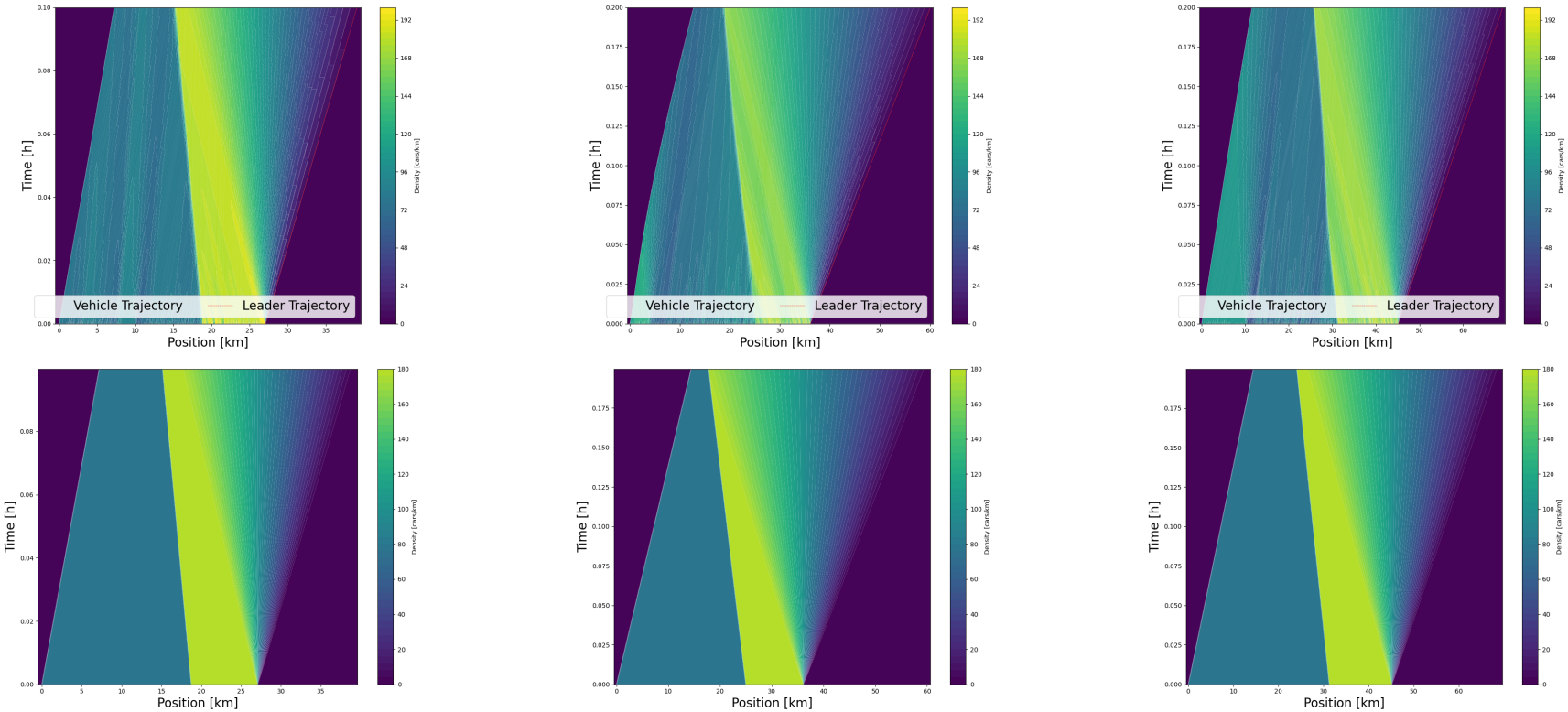

(a) $N = 3000$ (b) $N = 4000$ (c) $N = 5000$

Comparison of **reconstructed** and **macroscopic** densities
Top Reconstructed density from learning-based optimization
Bottom Macroscopic density from LWR PDE (Godunov scheme)

Stop-and-go wave scenario

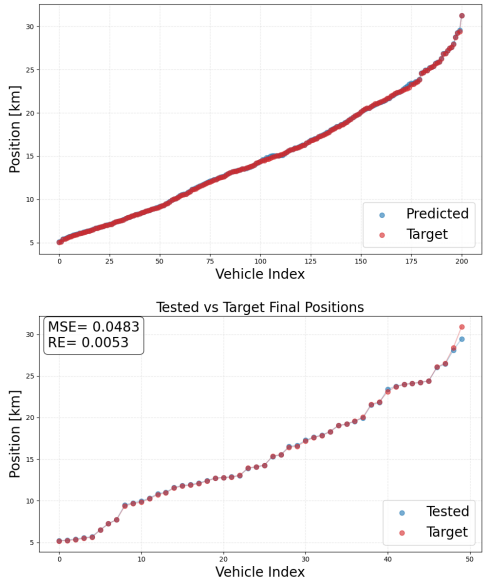

(a) $N = 2000$

Comparison of predicted and target final PV positions
Top Results from **training** procedure
Bottom Results on **test** sounds

Stop-and-go wave scenario

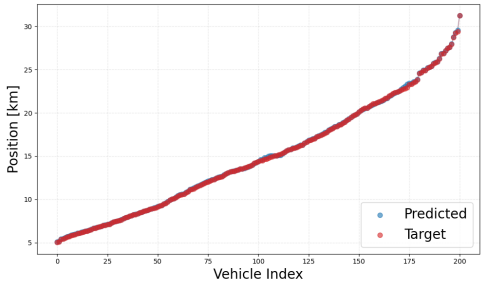

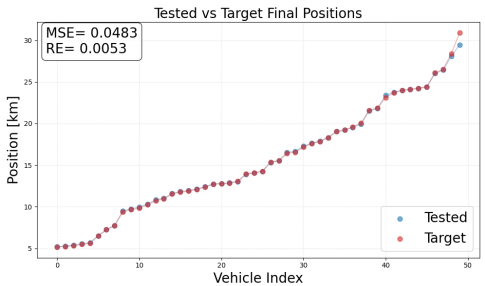

(a) $N = 2000$

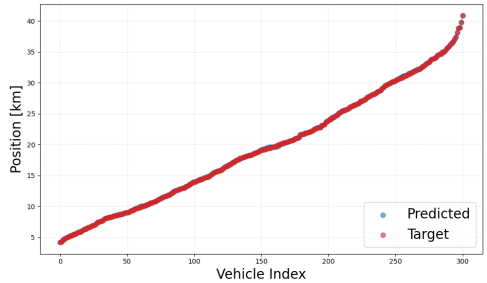

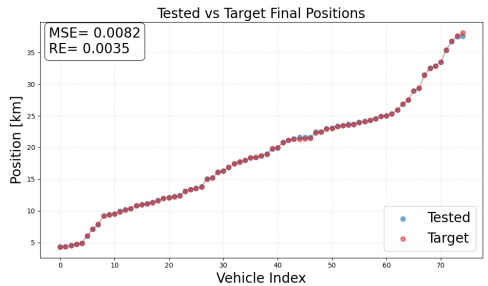

(b) $N = 3000$

Comparison of predicted and target final PV positions
Top Results from **training** procedure
Bottom Results on **test** sounds

Stop-and-go wave scenario

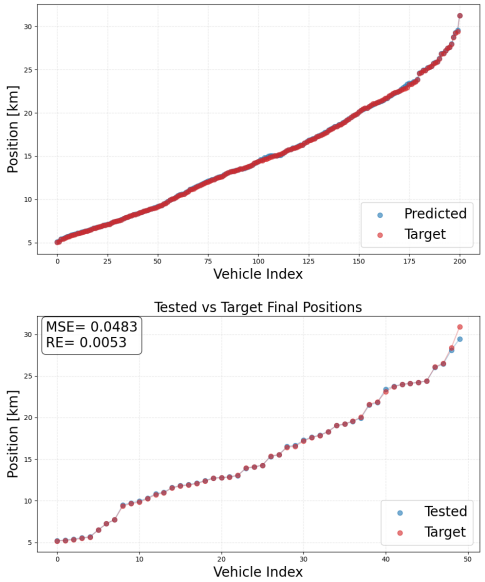

(a) $N = 2000$

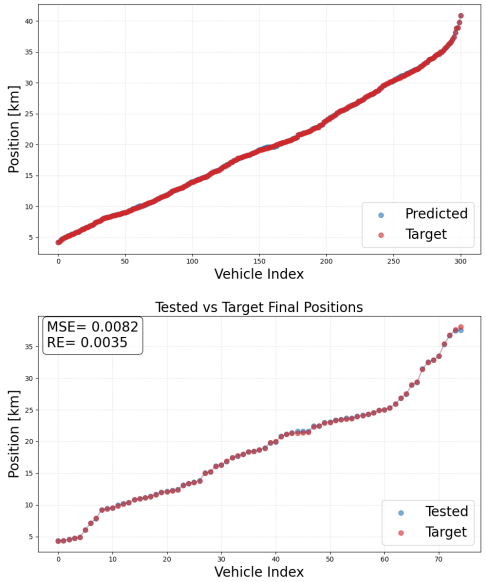

(b) $N = 3000$

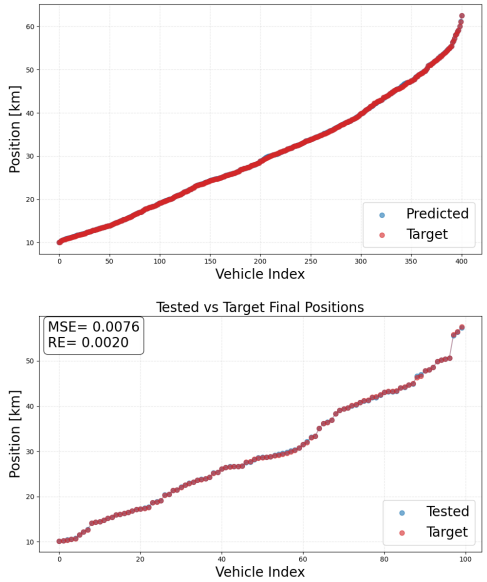

(c) $N = 4000$

Comparison of predicted and target final PV positions
Top Results from **training** procedure
Bottom Results on **test** sounds

Stop-and-go wave scenario

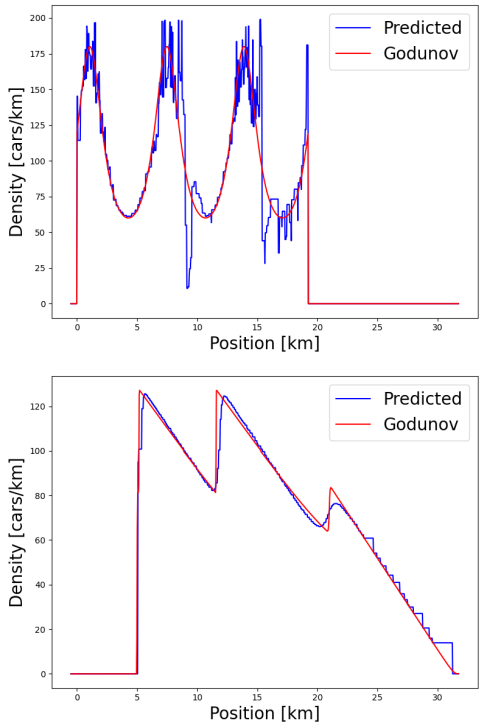

(a) $N = 2000$

Comparison of reconstructed and macroscopic densities
Top Initial densities
Bottom Final densities

Stop-and-go wave scenario

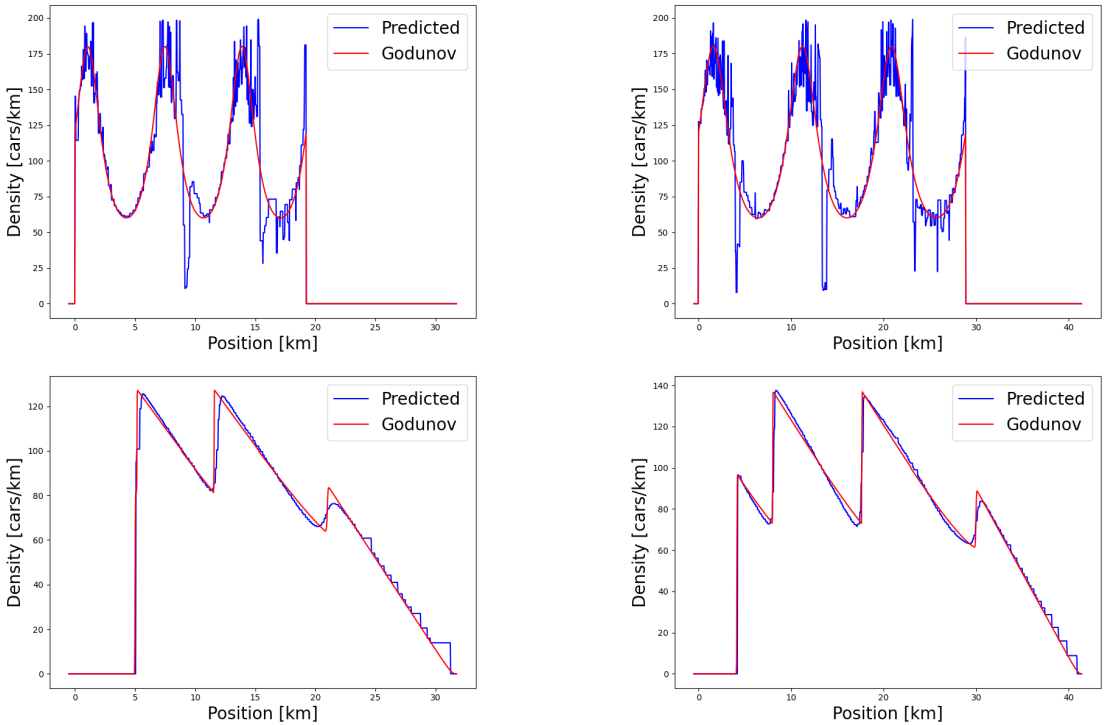

(a) $N = 2000$ (b) $N = 3000$

Comparison of reconstructed and macroscopic densities
Top Initial densities
Bottom Final densities

Stop-and-go wave scenario

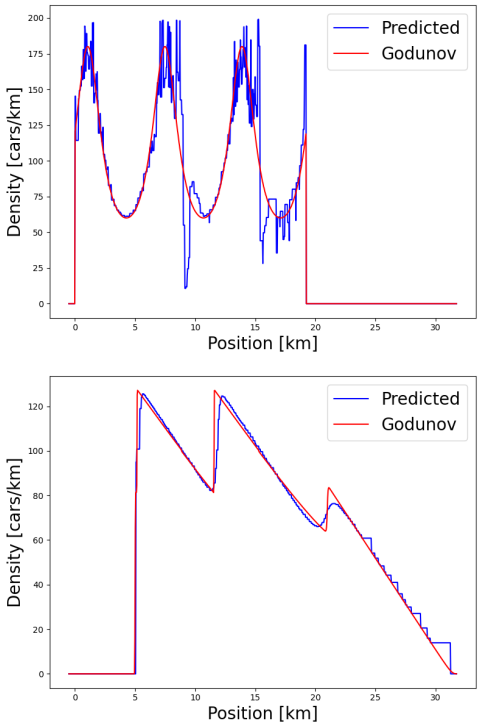

(a) $N = 2000$

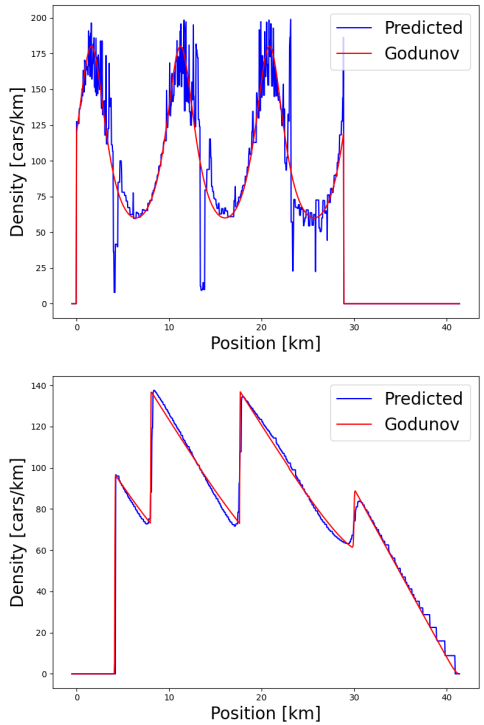

(b) $N = 3000$

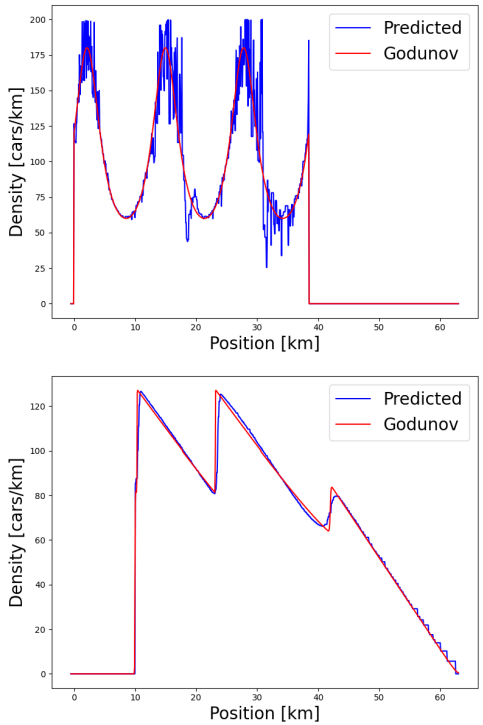

(c) $N = 4000$

Comparison of reconstructed and macroscopic densities
Top Initial densities
Bottom Final densities

Stop-and-go wave scenario

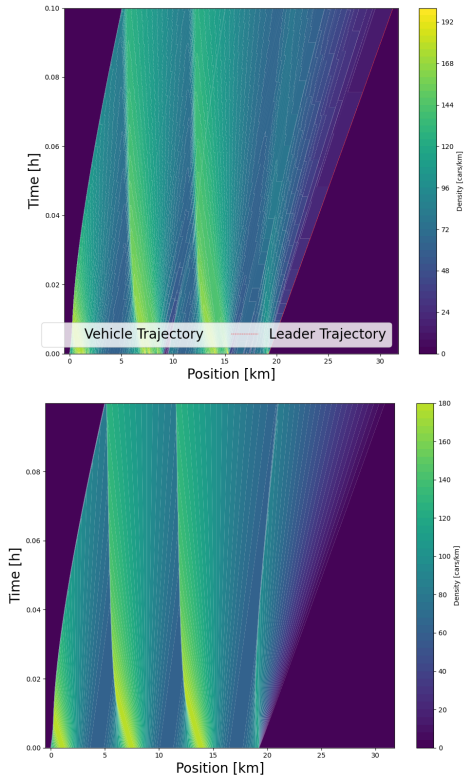

(a) $N = 2000$

Comparison of **reconstructed** and **macroscopic** densities
Top Reconstructed density from learning-based optimization
Bottom Macroscopic density from LWR PDE (Godunov scheme)

Stop-and-go wave scenario

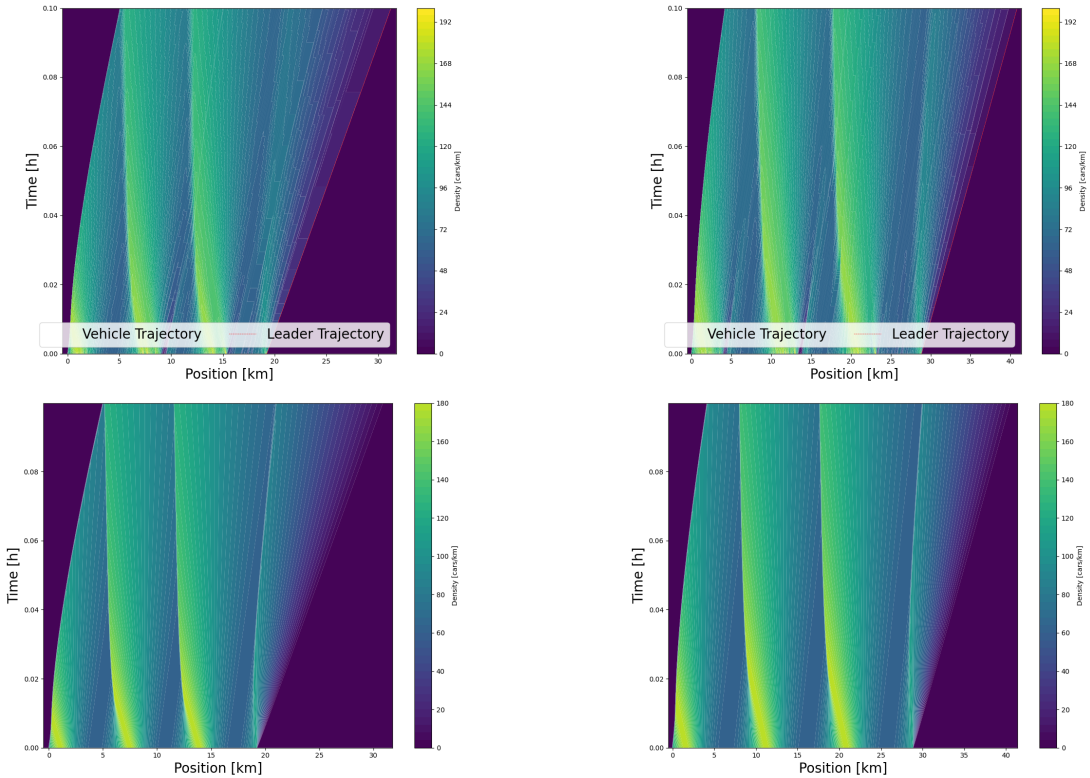

(a) $N = 2000$ (b) $N = 3000$

Comparison of **reconstructed** and **macroscopic** densities
Top Reconstructed density from learning-based optimization
Bottom Macroscopic density from LWR PDE (Godunov scheme)

Stop-and-go wave scenario

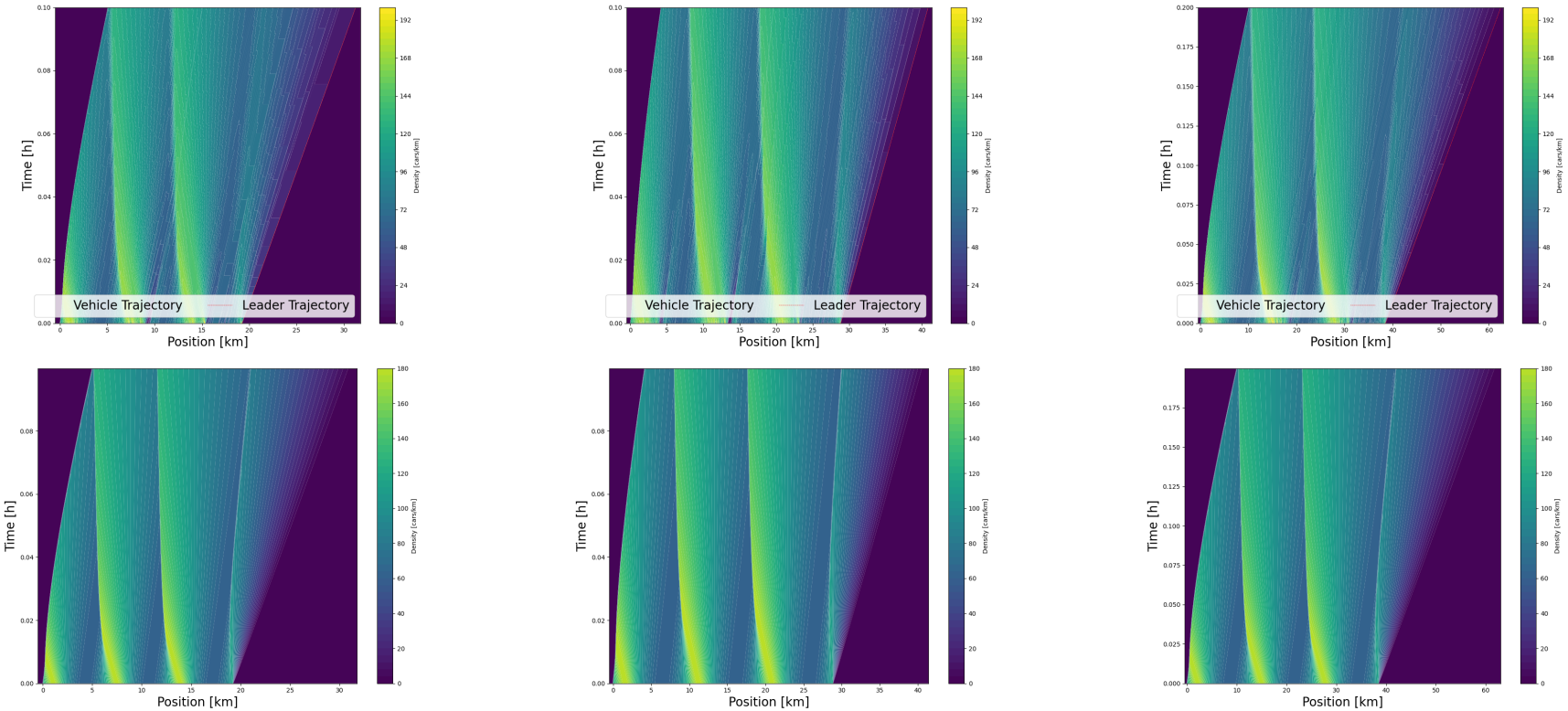

(a) $N = 2000$ (b) $N = 3000$ (c) $N = 4000$

Comparison of **reconstructed** and **macroscopic** densities
Top Reconstructed density from learning-based optimization
Bottom Macroscopic density from LWR PDE (Godunov scheme)

Table of Contents

Conclusion

Traffic State Reconstruction Approaches

- Model-Based Method
  ⇒ uses microscopic and macroscopic models
  ⇒ provides theoretical guarantees
  ⇒ struggles to capture real-world complexities
- Data-Driven Method
  ⇒ learns patterns directly from measurement data
  ⇒ derives system properties or predicts near-future states
  ⇒ requires extensive data for effectiveness
- Our Approach
  ⇒ combines models and data to address sparsity and improve realism
  ⇒ **Integrates physical priors with data observations**
  ⇒ achieves reliable traffic reconstruction with limited observations

Perspectives

- Conservation law with unilateral constraint[9] (toll gate)

$$\begin{cases} \text{LWR PDE (6) with} \\ f(\rho(t,0)) \leq q(t), \qquad t > 0. \end{cases} \tag{32}$$

- Conservation law with moving bottleneck[10] (slow vehicle)

$$\begin{cases} \text{LWR PDE (6) with} \\ f\left(\rho(t,y(t))\right) - \dot{y}(t)\rho(t,y(t)) \leq \frac{\alpha \rho_{\max}}{4 v_{\max}} \left(v_{\max} - \dot{y}(t)\right)^2, & t > 0, \\ \dot{y}(t) = \omega\left(\rho(t,y(t)_+)\right), & t > 0, \\ y(0) = y_0 \end{cases} \tag{33}$$

- Network[11] with a junction[12] J and N incoming roads and M outgoing ones

$$\begin{cases} \partial_t \rho_l(t,x) + \partial_x\left(f(\rho_l(t,x))\right) = 0, & t > 0, \quad x \in I_l, \quad l = 1, \dots, N+M \\ \rho_l(0,x) = \rho_{0,l}(x), & x \in I_l = [a_l, b_l], \quad l = 1, \dots, N+M \end{cases} \tag{34}$$

$\Rightarrow \sum_{i=1}^{N} f\left(\rho_i(t,(b_i)_-)\right) = \sum_{j=N+1}^{N+M} f\left(\rho_j(t,(a_j)_+)\right)$ (Rankine Hugoniot)

$\Rightarrow \sum_{i=1}^{N} f\left(\rho_i(t,(b_i)_-)\right)$ is maximized[13] s.t. $f\left(\rho_j(\cdot,(a_j)_+)\right) = \sum_{i=1}^{N} a_{j,i} f\left(\rho_i(\cdot,(b_i)_-)\right)$

[9] Colombo and Goatin 2007.
[10] Liard and Piccoli 2021.
[11] Monneau 2024.
[12] Coclite, Piccoli, and Garavello 2005.
[13] Garavello and Piccoli 2006.

References I

Baloul, N., A. Hayat, T. Liard, and P. Lissy (2025). "Traffic Flow Reconstruction from Limited Collected Data". In: *hal preprint hal-05042012v1*.

Barreau, M., M. Aguiar, J. Liu, and K. H. Johansson (2021). "Physics-Informed Learning for Identification and State Reconstruction of Traffic Density". In: *arXiv preprint arXiv:2103.13852*.

Coclite, G. M., B. Piccoli, and M. Garavello (2005). "Traffic Flow on a Road Network". In: *SIAM Journal on Mathematical Analysis* 36.6, pp. 1862–1886.

Colombo, R. M. and P. Goatin (2007). "A Well-Posed Conservation Law with a Variable Unilateral Constraint". In: *Journal of Differential Equations* 234.2, pp. 654–675.

Di Francesco, M., S. Fagioli, M. D. Rosini, and G. Russo (2016). "Follow-the-Leader Approximations of Macroscopic Models for Vehicular and Pedestrian Flows". In: *arXiv preprint arXiv:1610.06743*.

Di Francesco, M. and M. D. Rosini (2015). "Rigorous Derivation of Nonlinear Scalar Conservation Laws from Follow-the-Leader Type Models via Many Particle Limit". In: *arXiv preprint arXiv:1404.7062*.

Garavello, M. and B. Piccoli (2006). *Traffic Flow on Networks*. Vol. 1. Applied Mathematics. American Institute of Mathematical Sciences.

References II

Holden, H. and N. H. Risebro (2017). "The Continuum Limit of Follow-the-Leader Models: A Short Proof". In: *arXiv preprint arXiv:1709.07661*.

Liard, T. and B. Piccoli (2021). "On entropic solutions to conservation laws coupled with moving bottlenecks". In: *Communications in Mathematical Sciences* 19.4, pp. 1041–1068.

Liu, J., M. Barreau, M. Cicic, and K. H. Johansson (2020). "Learning-Based Traffic State Reconstruction Using Probe Vehicles". In: *arXiv preprint arXiv:2011.05031*.

Monneau, R (2024). "Structure of Riemann solvers on networks (preliminary version)". In: *hal preprint hal-04764513v1*.